JCTC Journal of Chemical Theory and Computation

Article

pubs.acs.org/JCTC

Substituent Effects on Menshutkin-Type Reactions in the Gas Phase and Solutions: Theoretical Approach from the Orbital Interaction View

Lizhi Jiang,[†] Yuuichi Orimoto,[‡] and Yuriko Aoki*[,‡,§]

[†]Department of Molecular and Material Sciences, Interdisciplinary Graduate School of Engineering Sciences, Kyushu University, Kasuga Fukuoka 816-8580, Japan

[‡]Department of Material Sciences, Faculty of Engineering Sciences, Kyushu University, Kasuga Fukuoka 816-8580, Japan

[§]Group, CREST, Japan Science and Technology Agency (JST), Kawaguchi Center Building, 4-1-8 Honcho, Kawaguchi, Saitama 332-0012, Japan

Supporting Information

ABSTRACT: In this study, we developed a method to interpret the mechanism of acceleration for Menshutkin-type reactions in solutions theoretically, from the orbital interaction view, utilizing the through-space/bond (TS/TB) interaction analysis in the polarizable continuum model (PCM). Different method levels were tested to determine the substituent effects on the reactions of NH_3 attacking para-substituted benzyl bromide. The geometrical structures and Mulliken charge distributions were analyzed to elucidate the substituent effects on the S_N2 reaction center. The results of Mulliken charge analysis showed that the para-substituted benzyl group ($-C_6H_4Y$) received negative charge through the reaction process, and both electron-donating and electron-withdrawing substituents Y made $-C_6H_4Y$ groups receive greater charges. Solvent effects on the structures of transition states (T-S(s)) were significant. The structures of T-S(s) were found to be exhibiting longer bond lengths in solutions, especially in polar solvents such as water. Our TS/TB-PCM analysis method can predict the substituent effects in solutions by evaluating contributions from orbital interactions in question. The orbital interaction analysis results revealed that the key orbital interactions for stabilizing the T-S(s) of the systems with substituents Y = NH_2 and NO_2 in water were $n(NH_2)-\pi^*(ph)$ (ph = phenyl) and $\pi(ph)-\pi^*(NO_2)$ interactions, respectively. Stronger interactions between $\pi^*(ph)$ and $\sigma^*(C_\alpha\text{-Br})$ occurred because of the $n(NH_2)-\pi^*(ph)$ and $\pi(ph)-\pi^*(NO_2)$ interactions that resulted when para-substituents $-NH_2$ and $-NO_2$, respectively, were added to the system. These stronger $\pi^*(ph)-\sigma^*(C_\alpha\text{-Br})$ interactions stabilized the transition state and enabled the Br leaving group to leave more easily.

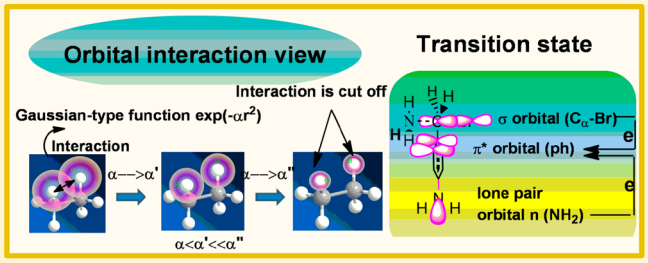

INTRODUCTION

The stability and other various properties of a molecule strongly depend on the intramolecular and intermolecular orbital interactions caused by orbital overlap. By evaluating the orbital interactions, the key part that contributes to the reactivity or other chemical properties of a molecule becomes clear, which can give helpful insight into experiments.[1−13] The concept of through-space/bond (TS/TB) orbital interactions proposed by Hoffmann et al.[1,2] has been applied to various fields in chemistry, such as probing the mechanism of charge transfer,[10,14−16] energy transfer,[17] and stereoelectronic effects.[11,18] Imamura et al. developed the TS/TB orbital interaction analysis method at the ab initio level, making it possible to evaluate the orbital interaction quantitatively.[7] In our previous study,[11] the analysis was developed extended to be based on natural bond orbital (NBO)[19] basis set to elucidate the stereoelectronic effects on the total energies and reactivity of molecules in the gas phase.

This study interprets the mechanism of acceleration for reactions from the orbital interaction perspective, especially in solutions. The mechanism and factors that influence S_N2 reaction rates have intrigued chemists for a long time.[20−36] In S_N2 reactions, it was proposed that the π orbitals of the substituents can act as electron donors or electron acceptors to stabilize the transition states (T-S(s)) by stereoelectronic interactions, and, hence, accelerate the reactions.[37] The π-orbital character of the phenyl (ph) group of benzyl bromide can vary to a great extent, depending on substituents.[37] In addition, an unusual phenomenon for para-substituted benzyl compounds has been experimentally observed. They react faster than unsubstituted benzyl compounds, and the phenomenon occurs, irrespective of the substituent being electron-donating or electron-withdrawing.[37,38] In addition to the substituent effects, the influence of solvent is also

Received: May 31, 2013
Published: July 22, 2013

dx.doi.org/10.1021/ct4006163 | J. Chem. Theory Comput. 2013, 9, 4035−4045

profound[20,22,25,31,39] in S_N2 reactions. Bimolecular reactions usually behave differently in the gas phase than in solutions, because of the solvation effects on the molecules. However, the reaction rates are directly determined by the extent of solvation of reactants and T-S(s) in the solutions. In normal S_N2 reactions, the nucleophiles, with a negative charge of the reactants, are stabilized more than the T-S(s) by polar solvents, which causes the activation barriers in the solution phase to be higher than those in the gas phase.[22,25] In Menshutkin-type S_N2 reactions,[40] as shown in Figure 1, on the other hand, the T-S(s)

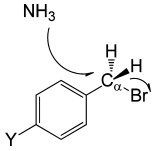

Figure 1. Model for the Menshutkin-type S_N2 reactions of para-substituted benzyl bromide attacked by NH_3.

prefer the existence of polar solvents and are preferentially stabilized, leading to the acceleration of these reactions. Some previous studies investigated and compared the mechanisms of the two types of S_N2 reactions in solutions (normal and Menshutkin).[20] In this study, our interest is on how the orbital interactions are influenced by the solutions in the process of tuning the reaction reactivity; thus, we chose to study the Menshutkin reactions, which prefer the existence of solvents. Concerning the mechanism of substituent effects in solutions, some studies theoretically examined the solvent effects by using the polarizable continuum model (PCM).[22,41−46] However, most of them focused solely on the solvent effects on the reactivity of molecules, and an explanation for the unusual phenomenon of para-substituted benzyl bromide in the S_N2 reactions was not discussed. In solution, how are the donating and accepting abilities of the π-orbitals in the phenyl ring varied by changing the substituents? The TS/TB interaction analysis can be an effective tool for investigating such issues.

In this study, we developed the TS/TB-PCM method by combining TS/TB analysis with the PCM in GAMESS software.[47] The treatment makes it possible to estimate the contribution of specific orbital interactions to stabilize the system in solutions. The mechanism of the effects of substituents Y on stabilizing the T-S(s) will be illuminated from an orbital interaction view by our TS/TB-PCM method.

THEORETICAL METHODOLOGY AND COMPUTATIONAL DETAILS

TS/TB Orbital Interaction Analysis. Treatment with the TS/TB orbital interaction method enables us to estimate the contributions of the specific orbital interactions in a molecule.[9,11] The procedures of the method are as follows.

In the procedure, the contributions of orbital interactions are examined by deleting the interactions from the systems and are evaluated in terms of the energy difference before and after the deletions. The orbital interactions that must be cut off are calculated using the basis sets with extremely large artificial exponents (Figure 2). When the exponents of the orbital functions that correspond to different atoms increase to an extremely large value, the overlap integrals $S_{rs} = \int \chi_r(1)\chi_s(1)\, d\tau_1$, the kinetic energy integral T_{rs}, and the nuclear-electron attractive integral V_{rs} become zero. Simultaneously, all of the off-diagonal elements of the two-electron integrals (rsltu) =

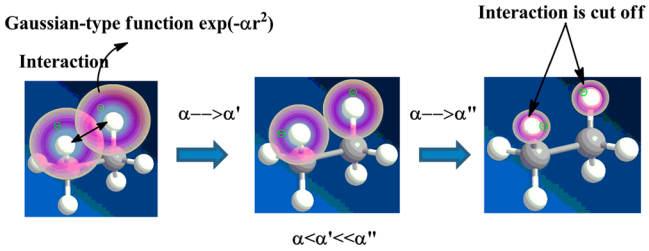

Figure 2. Deletion of a specific interaction between orbitals in the TS/TB method.

$\int\int \chi_r(1)\chi_s(1)(1/r_{12})\chi_t(2)\chi_u(2)\, d\tau_1\, d\tau_2$ become zero as the exponents of χ_r and χ_s become increasingly large. As a result, the specific orbital interactions between χ_r and χ_s have been deleted from the systems by this procedure.

Polarizable Continuum Model (PCM). In the PCM solvent model, a solute molecule is placed within a cavity, and the cavity is surrounded by a dielectric continuum. The interaction potential V_{MS} between the solute molecule and solvent is defined as[48]

$$V_{MS} = \int_s V(s)\sigma(s)\, ds \tag{1}$$

where $V(s)$ is the electrostatic potential of the solute molecule calculated on the cavity surface, s; $\sigma(s) = \sigma^N(s) + \sigma^e(\rho;s)$ is the surface charge density, which is partitioned into contributions from the nuclei and electrons of the solute, $\sigma^N(s)$ and $\sigma^e(\rho;s)$, respectively. $\sigma^e(\rho;s)$ depends on the electron density ρ of the solute molecule. The surface charge density $\sigma(s)$ is a function of ρ, the cavity, and the solvent dielectric constant (ε_s).

In the program, the cavity surface is divided into M small portions (tesserae) of area a_m to compute V_{MS}. For the mth portion, the induced charge is treated as a point charge $q_m = a_m\sigma(s_m)$, and it is placed at the geometrical center of the portion. For the integral equation formalism (IEF) PCM, the charges q_m can be obtained by solving the matrix equation:

$$q^z = -Q(\varepsilon)V^z \qquad (z = e, N) \tag{2}$$

where $Q(\varepsilon)$ is a square matrix; it depends on the solvent dielectric constant ε and the geometrical parameters for the molecular cavity. V is the vector that collects (electronic or nuclear) potential values on the portion. After this treatment, the surface integrals in eq 1 can then be obtained by the summations over M portions.

Through-Space/Bond Orbital Interaction Analysis Combined with the Polarizable Continuum Model (PCM). In the Hartree−Fock (HF) method, the PCM treats the solvent effects on the solute by adding the solute−solvent interaction potential V_{MS} as a perturbation to the Hamiltonian Fock matrix. Thus, in the analysis of PCM solvent effects, the Hamiltonian in the HF equation can be written as follows:[49,50]

$$(F^0 + V_{MS})\psi = E\psi \tag{3}$$

where F^0 is the Hamiltonian Fock matrix in a vacuum, and ψ is the solute wave function in solution. F^0 can be expressed as $F^0 = H^{core} + G$. Here, H^{core} is the sum of the kinetic energy integrals T and the nucleus−electron potential integrals V (one electron integrals), and G is the sum of the electron−electron potential energy integrals (two electron integrals). One part of the interaction potentials $V^N_{MS} = \int_s V(s)\sigma^N(s)\, ds$, which is caused by the nuclei of the solute, is added to H^{core}. The other electron-density-dependent part $V^e_{MS} = \int_s V(s)\sigma^e(\rho;s)\, ds$, which is caused

dx.doi.org/10.1021/ct4006163 | J. Chem. Theory Comput. 2013, 9, 4035−4045

by electrons of the solute, is added to the two-electron part G to form the Fock matrix in the HF calculations.

In our TS/TB orbital interaction analysis,[11] two files (File-1 and File-2) are used for storing integrals that are calculated using a normal basis set and an artificial basis set, respectively. The AO basis set was changed to the NBO basis to define the specific orbitals to be cut off in the large basis set. A flowchart describing the TS/TB-PCM is shown in Figure 3. In these

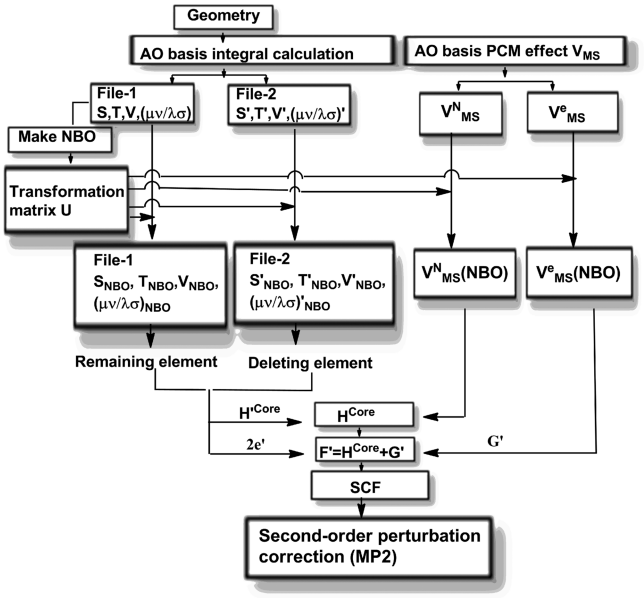

Figure 3. Flowchart of the TS/TB-PCM method.

steps, the NBO-based overlap matrix S_{NBO} can be constructed by being left multiplied with an orthogonal transformation matrix U and then right multiplied with the reverse of the transformation matrix U^{-1}, $S_{NBO} = US_{AO}U^{-1}$. Moreover, the NBO-based kinetic energy integral matrix T_{NBO}, nucleus−electron potential integrals V_{NBO}, and the two-electron integrals $(\mu\nu|\lambda\sigma)_{NBO}$ can be obtained by the same actions. The details of the NBO-based TS/TB orbital interaction analysis are described in our previous study.[9,51] The original solute−solution interaction potential V_{MS} matrix that is calculated in the PCM is originally based on AO. There will be problems if the AO-based V_{MS} is directly added to the NBO-based Fock matrix in the TS/TB orbital interaction analysis procedure. One strategy is to adopt the same basis transformation action on the term V_{MS}; thus, the same basis transformation action was adopted for the term V_{MS} to change from the AO basis to the NBO basis. First, the electrostatic potential values V^N (eq 2) that are computed on tesserae for the nuclei-induced interactions were transformed to the NBO basis, and the $Q(\varepsilon)$ matrix was also transformed. Second, the electron-induced potentials V^e_{MS} were changed to the NBO basis. Notably, V^e (eq 2) is dependent on the electron density, and it is important to point out that the electron density (D) in the self-consistent field (SCF) procedure of the solute has already been transformed to the NBO basis in the TS/TB treatment. Thus, in this part, only the $Q(\varepsilon)$ matrix in the electron-induced potentials needed to be transformed. After basis transformation, the item V^N_{MS}(NBO) was added to H^{core}, and the item V^e_{MS}(NBO) was added to G in the SCF procedure to form the Fock matrix.

To test the correction of the energy that was estimated in the PCM at the NBO basis, we used ethylene and the T-S of benzyl bromide as examples to express the energy difference. For ethylene, the difference between the energies calculated at the AO basis and the NBO basis was $\sim 1.0 \times 10^{-7}$ a.u. For the T-S of benzyl bromide, the energy difference was $\sim 1.0 \times 10^{-5}$ a.u. Both of the energy differences are under the SCF convergence limitation. Thus, our developed TS/TB-PCM method can be used to investigate energy differences at the NBO basis.

Activation Strain Analysis. Bickelhaupt et al.[52−54] proposed a fragment-based approach (activation strain model) to illustrate the factors that control chemical reactions. In S_N2 reactions between [Pd] and CH3X, the reaction mechanism, which is affected by the nature of the C−X bond strength and solvent effects, is well-interpreted by this fragment-based method.[52] Here, we use this method to test if the para-substituent effects are shown in terms of structure deformation. The activation energy $\Delta E^{\ddagger}$ is expressed by the strain energy $\Delta E^{\ddagger}_{strain}$ and the interaction energy $\Delta E^{\ddagger}_{in}$ and is shown in the following equation:

$$\Delta E^{\ddagger} = \Delta E^{\ddagger}_{strain} + \Delta E^{\ddagger}_{in} \quad (4)$$

As shown in Figure 4, $\Delta E^{\ddagger}_{strain}$ is defined as the energy change from the optimized separate reactants, relative to that of the

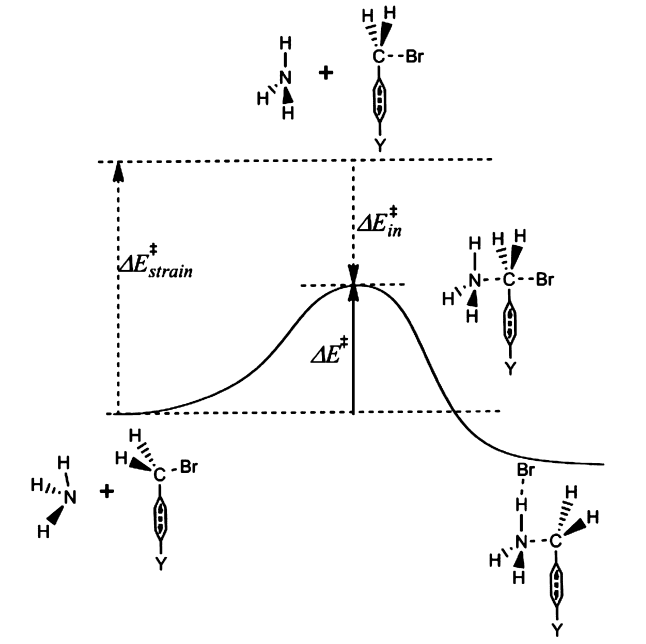

Figure 4. Activation strain model for a Menshutkin reaction.

deformed reactants in the activated T-S complex. $\Delta E^{\ddagger}_{in}$ expresses the energy change from the deformed reactants to the T-S complex.

Computational Details. The structures of the separate reactants, reactant complex intermediates (C_{react}), and product complexes (C_{prod}) were optimized at the HF, B3LYP, and MP2 levels to compare whether the level is sufficient. The 6-31G, 6-31G(d, p), and 6-31+G(d) basis sets were selected to compare the effects of polarization and diffusion functions in the basis sets on the geometrical structure and activation energy. The T-S(s) were also searched and optimized at the same levels. Intrinsic reaction coordinate (IRC) calculations, which define the reaction path, were also carried out to verify the minima

dx.doi.org/10.1021/ct4006163 | J. Chem. Theory Comput. 2013, 9, 4035−4045

and the T-S(s). The frequency harmonic vibrational analysis was performed to determine the structures of stable separate reactants, products, intermediates, and the T-S(s). The activation energies E_a were defined as the difference between the energies of T-S(s) and the reactant intermediates; the energies E_a were corrected by zero-point vibrational energies. All of the calculations were carried out using the GAUSSIAN 09 package.[55] The NBO-based TS/TB-PCM method that we developed has been incorporated into the GAMESS program package.[47] The NBO-based TS/TB-PCM method for examining orbital interactions in solvents was performed at the MP2/6-31+G(d) levels.

RESULTS AND DISCUSSION

Substituent Effects on the Stabilization of the Transition State in the Gas Phase. Some previous studies have tested the basis set effects for calculations of reaction barrier heights.[35,56] To present the substituent effects as well, the results calculated by HF, post-HF (MP2), and DFT (B3LYP) methods were compared here. The different trends of the substituent effects on the activation energies shown in Figure 5 imply that the substituent effects obviously depend on

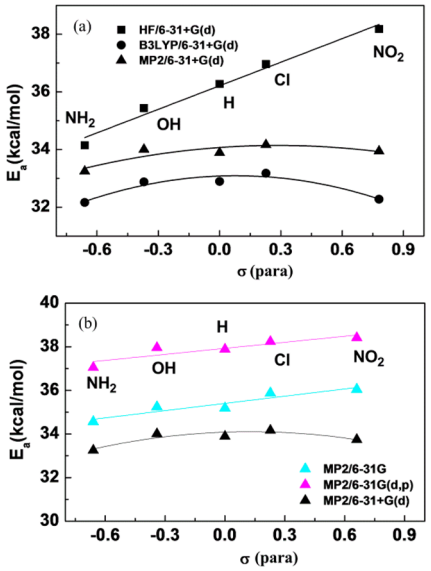

Figure 5. Relationship of activation energies (E_a) of the systems with the Hammett parameter sigma (σ) of the para-substituent Y (a) at the HF, B3LYP, and MP2 levels, and (b) at MP2 level, using different basis sets.

the level of theory. At the HF level, the activation energies increased when substituents were electron acceptors but decreased when the substituents were replaced by electron donors. On the other hand, the relationships between the activation energy and the Hammett constant sigma (σ)[38,57] of the para substituents were not linear but curved at both the MP2 and B3LYP levels. The phenomenon observed at the MP2 (Figures 5a and 5b) and B3LYP (Figure 5a) levels agreed with previous experimental results.[37] Based on the experimental results, both electron-donating and electron-withdrawing para-substituents accelerated the reaction. Electron correlation effects are also important in the calculation of activation energies, as a significant difference is observed when comparing the results obtained at the HF and MP2 levels. The HF level is not sufficient to estimate the substituent effects in this case. The basis set effect is also significant for defining the influence of substituents. The basis sets 6-31G, 6-31G(d, p), and 6-31+G(d) were chosen for comparing the calculation results. The diffusion functions in the basis set were found to be necessary for describing the correction energies of T-S(s), as MP2/6-31+G(d) reproduced experimental data. The detailed data of the differences in the activation energies are listed in Table S1 in the Supporting Information. The results in Figure 5b indicate that the basis set 6-31+G(d) is sufficient to interpret the substituent effects. Moreover, previous studies pointed out that the structures obtained at the 6-31+G(d) and 6-31++G(d, p) levels gave small differences.[24,58] Thus, the following analyses of the mechanisms were based on the MP2/6-31+G(d) calculations.

Dodd et al.[59] discussed a method to more accurately account for the potential wells in ion molecule reactions. Some early studies treated the activation energy as the difference between T-S(s) and the separate reactants,[60] in which the solvation of the reactant complex is voided. In this study, the activation energy is defined as the difference between T-S(s) and reactant complexes (reactant intermediate, C_{react}). For comparison, both the relative energies between T-S(s) and separate reactants and those between C_{react} and separate reactants are listed in Table 1. The reaction process is shown in Figure 6, and the relative energies of each calculated state are marked. In the MP2/6-31+G(d) calculations, two types of reactant complexes (C_{react} and $C_{react}(2)$) were obtained.[61] The former complex C_{react} positions the attacking group NH_3 on the same side as the leaving group Br, because hydrogen bonds are formed between the Br atom and the H atom in NH_3 and also between the N atom and the H atom that is attached to C_α. The latter complex $C_{react}(2)$ positions NH_3 on the opposite side of the benzene ring plane relative to Br. E_a in the graph is the difference between the energies of T-S and C_{react}, and E_{a2} is the difference between the energies of T-S and $C_{react}(2)$. Although the energies of C_{react} are lower than those of $C_{react}(2)$, the trend of activation energies within the C_{react} and $C_{react}(2)$ series were the same. The electron-donating $-NH_2$ group, as well as the electron-withdrawing $-NO_2$ group, stabilized the T-S. The activation energies of para-substituted benzyl bromides in Menshutkin reactions were consequently reduced. For the product complexes, it was easy to form the salt product complex C_{prod} from the structure of $C_{prod}(2)$. C_{prod} can be obtained through IRC calculations. Because we were interested in studying the effects of substituent on the reactivity, the discussion of the product C_{prod} is concise.

Electron-transfer activities in the reactions were investigated to illuminate the effects of para-substitution on the reactivity of benzyl bromide. It was interesting to find that the para-substituent Y adjusts the reactivity of benzyl bromide by tuning the electron activities in the reaction process. Here, the electron transfer within the molecular structure is denoted by "relative reduced charge", Δe. The value of Δe is defined as the Mulliken atomic charges in the T-S(s) minus that in the separate reactant. For example, the charge transfer in the $-C_6H_4Y$ group in benzyl bromide is defined as $\Delta e(-C_6H_4Y) = e_{T\text{-}S}(-C_6H_4Y) - e_{sep\text{-}react}(-C_6H_4Y)$; $e_{T\text{-}S}(-C_6H_4Y)$ is the sum of the Mulliken charges on the atoms in the $-C_6H_4Y$ group of the T-S, and $e_{sep\text{-}react}(-C_6H_4Y)$ is the sum of Mulliken charges on the atoms in the $-C_6H_4Y$ group of the separate reactants. Figure 7 shows the relationship of the Δe of the substituted phenyl moieties ($-C_6H_4Y$) with the Hammett parameter (σ). The curve of Δe for the $-C_6H_4Y$ group indicates that all of the

dx.doi.org/10.1021/ct4006163 | J. Chem. Theory Comput. 2013, 9, 4035−4045

Table 1. Relative Energies of Benzyl Bromide Reactant Complexes (C_{react}) and Transition States (T-S(s)) in the Gas Phase and Solutions at the MP2/6-31+G(d) Level[a]

	Relative Energy (kcal/mol) in Gas					Relative Energy (kcal/mol) in Solutions									
						In Water					In Benzene				
Y	R^b	$C_{react}{}^b$	T-S^b	$C_{prod}{}^b$	E_a	R^b	$C_{react}{}^b$	T-S^b	$C_{prod}{}^b$	E_a	R^b	$C_{react}{}^b$	T-S^b	$C_{prod}{}^b$	E_a
NH_2	0	−4.62	28.62	−2.72	33.25	−18.57	−21.35	−5.20	−47.73	16.15	−7.87	−12.38	10.26	−24.51	22.81
OH	0	−4.85	29.15	−2.57	34.00	−19.04	−21.84	−5.17	−48.26	16.66	−8.18	−12.74	10.77	−24.47	23.51
CH_3	0	−4.87	28.64	−3.17	33.52	−13.52	−16.40	0.24	−42.94	16.63	−5.76	−10.13	12.97	−22.40	23.10
H	0	−4.88	29.01	−2.59	33.89	−13.48	−16.36	0.47	−42.87	16.84	−5.73	−10.40	13.26	−22.14	23.65
F	0	−5.18	29.30	−1.93	34.48	−15.06	−17.92	−0.94	−42.39	16.98	−6.51	−11.31	12.64	−22.25	23.96
Cl	0	−5.37	28.79	−2.05	34.17	−14.38	−17.23	−0.34	−48.55	16.83	−6.16	−11.00	12.68	−21.80	23.67
CN	0	−5.69	28.62	−1.35	34.12	−19.31	−22.17	−5.40	−48.48	16.76	−8.44	−13.38	10.30	−23.30	23.69
NO_2	0	−5.64	28.31	−0.69	33.94	−19.58	−22.33	−5.66	−48.30	16.67	−8.35	−13.34	10.29	−22.66	23.63

[a]Legend: Y, substituent; *R*, separate reactant; C_{react}, reactant complex; T-S, transition state; and E_a, activation energy. [b]Relative energies with the separate reactants in the gas phase.

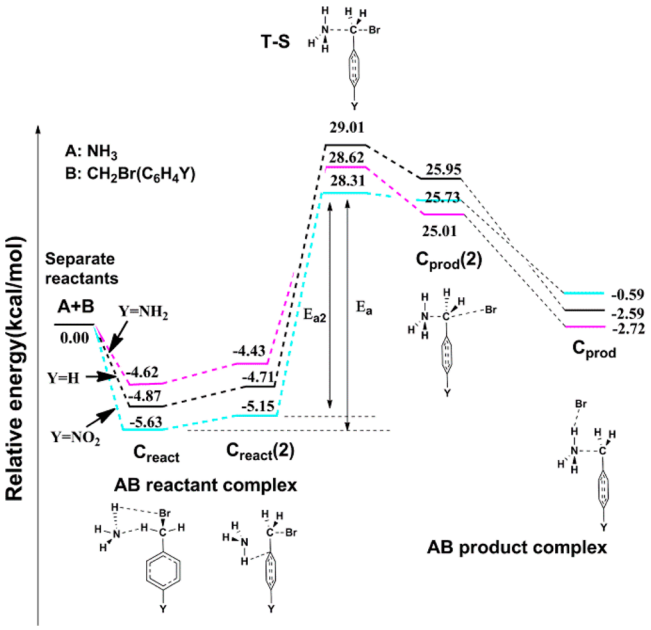

Figure 6. Relative energies of the reactant complex (C_{react} and $C_{react}(2)$), transition state (T-S(s)), and product complex (C_{prod} and $C_{prod}(2)$) with separate reactants of systems with different substituents Y in the gas phase.

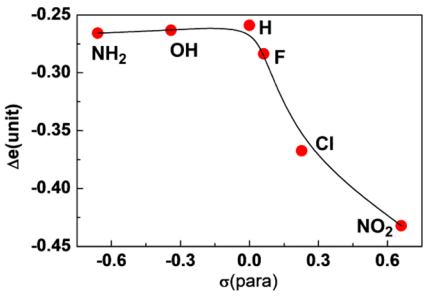

Figure 7. Relationship of Δe for the $-C_6H_4Y$ group of the systems with the Hammett parameter (σ) of para-substituent Y.

electron-donating substituents Y (such as NH_2 and OH) and electron-withdrawing substituents (such as NO_2 and Cl) enabled the $-C_6H_4Y$ group to receive electrons from the central carbon (C_α) group during the reaction process, as shown in Figure 7. That is, the $-C_6H_4Y$ group works as an electron-withdrawing group in the reaction process. Importantly, all types of para-substituents Y (electron-donating or electron-withdrawing) encouraged the ph group, as a whole, to accept more electrons, although the difference was marginal between systems with electron-donating Y groups and unsubstituted benzyl bromide (Table 2). This behavior may be ascribed to a stronger orbital interaction between the ph group and C_α when introducing para-substituents. This mechanism was further explored by the TS/TB orbital interaction analysis in the following investigation.

Table 2. Mulliken Charge Distributions in the Transition States (T-S(s)) and the Relative Reduced Charge Δe for Para-substituted Benzyl Bromide at the MP2/6-31+G(d) Level

	Mulliken Charge of the T-S(s) (unit)		Relative Reduced Charge Δe (unit)	
Y	$e_{T\text{-}S}$ (C_α)	$e_{T\text{-}S}$ ($-C_6H_4Y$)	Δe (C_α)	Δe ($-C_6H_4Y$)
NH_2	0.329	0.128	0.507	−0.265
OH	0.315	0.132	0.505	−0.263
H	0.293	0.134	0.518	−0.261
F	0.325	0.102	0.517	−0.283
Cl	0.394	0.011	0.585	−0.367
NO_2	0.500	−0.139	0.626	−0.432

Solvent Effects on the Reactivity of Para-substituted Benzyl Bromide. Solvent effects were remarkable for the reactions of NH_3 attacking para-substituted benzyl bromide. Polar (water) and nonpolar (benzene) solutions were both considered in the following solvent effects analyses. To clearly illustrate the solvent effects on the reaction barrier, the significance of the effects on separate reactants, C_{react}, T-S(s), and C_{prod} for the systems with Y = H, NH_2, and NO_2 are compared in Figure 8. The energies for other systems are listed in Table 1. Obviously, a polar solvent (water, blue line) stabilized these structures much more than a nonpolar solvent (benzene, green line). In water, the differences between separate reactants and C_{react} were very small. These results agree with previous experimental and theoretical studies;[25] the T-S(s) are stabilized much more than the reactants of Menshutkin reactions in solutions. In the gas phase, the energies of C_{prod} were slightly lower than those of separate reactants and were higher than C_{react}. However, the C_{prod} were stabilized more than C_{react} by solutions, especially by polar solvents, as shown in Figure 8; this may be another factor for

dx.doi.org/10.1021/ct4006163 | J. Chem. Theory Comput. 2013, 9, 4035−4045

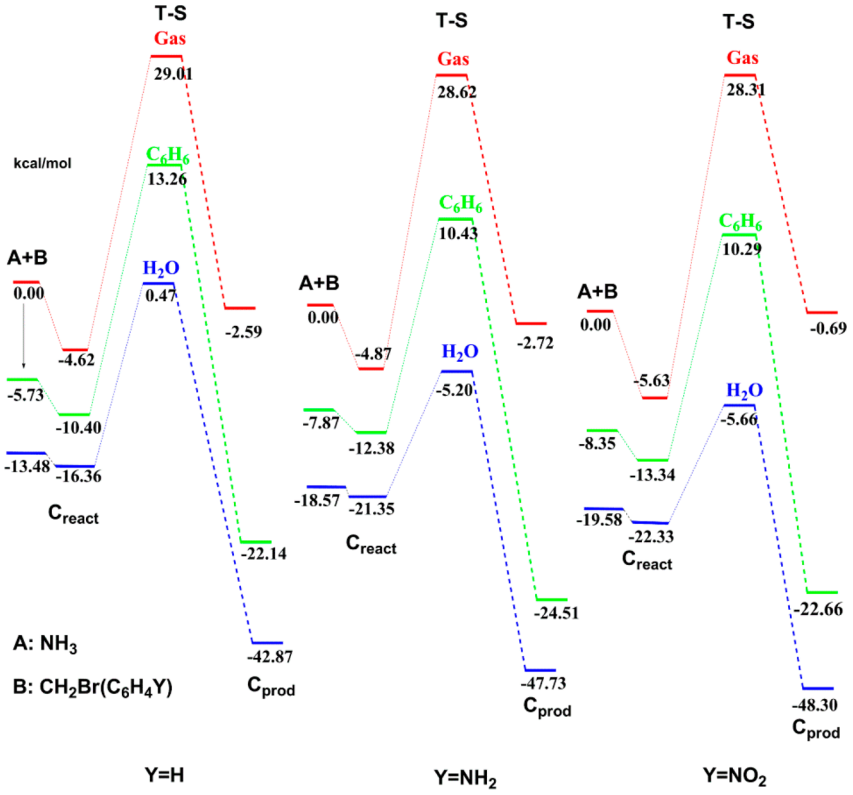

Figure 8. Polar and nonpolar solvent effects (water and benzene) on the energies for separate reactants (A + B), reactant complexes (C_{react}), transition states (T-S(s)), and product complexes (C_{prod}) of the systems with different Y (H, NH_2, and NO_2).

Table 3. Some Geometrical Structure Parameters of the Transition States (T-S(s)) in the Gas Phase and Solutions at the MP2/6-31+G(d) Level

	In Gas				In Solutions							
					Water				Benzene			
Y	N...C_α (Å)	C_α···Br (Å)	C_α–C_β (Å)	∠NC_αBr (°)	N···C_α (Å)	C_α···Br (Å)	C_α–C_β (Å)	∠NC_αBr (°)	N···C_α (Å)	C_α···Br (Å)	C_α–C_β (Å)	∠NC_αBr (°)
NH_2	1.904	2.604	1.465	171.97	2.286	2.471	1.445	165.73	2.087	2.525	1.456	168.56
OH	1.894	2.598	1.468	172.25	2.242	2.429	1.456	167.61	2.071	2.509	1.461	169.24
CH_3	1.890	2.590	1.470	173.41	2.227	2.411	1.461	168.80	2.062	2.496	1.464	170.62
H	1.885	2.588	1.472	173.18	2.212	2.399	1.465	169.06	2.054	2.490	1.467	170.51
F	1.885	2.589	1.471	173.09	2.212	2.400	1.464	169.15	2.055	2.492	1.466	170.38
Cl	1.883	2.587	1.471	173.88	2.208	2.395	1.465	169.77	2.052	2.487	1.467	171.10
CN	1.876	2.578	1.471	175.54	2.194	2.382	1.468	171.32	2.041	2.475	1.469	172.70
NO_2	1.878	2.575	1.471	175.96	2.189	2.376	1.469	171.74	2.039	2.471	1.469	173.05

the preference of a solution in Menshutkin reactions. It should be mentioned that temperature effects were not considered; all of the calculations were performed at 0 K, and no thermal corrections were performed. The results that consider the thermal free energies at 298 K and 1 atm pressure are given in Table S2 in the Supporting Information. The trend of the activation energies with thermal free energy corrections was similar to the results obtained at 0 K. Since transition states are sensitive to structural features, the solvent effects on the structural parameters of the T-S(s) were analyzed. Table 3 shows the difference between the geometrical structure parameters in gas and in solutions. The geometrical structure parameters were strongly related to polarization by solutions. For the T-S(s), the N···C_α distances became longer, and the C_α···Br distances became shorter in the solutions (Figure 9a). The distances of the partial bonds changed to a greater extent in water than in benzene. Also, the N···Br distances became larger in solutions, as shown in Figure 9b. In gas and solutions, the Hammett plots of the bond lengths showed the same trends, where the structures changed to be tighter (exhibited shorter bond lengths) when substituents became more electron-withdrawing. It is found that the structures became looser (exhibited longer bond lengths) in solutions, compared with those in the gas phase, especially in water. The changes in the geometrical structures indicate that it is easier to form the transition state in polar solvents. This phenomenon can be explained as Hammond postulate, that is, the reaction becomes more exothermic and the T-S becomes more reactant-like in solution.[46,62]

Activation Strain Analysis in the Gas Phase and Solutions.[52,53] In this activation strain model,[52] the activation energy $\Delta E^{\ddagger}$ is divided into the activation strain energy

dx.doi.org/10.1021/ct4006163 | J. Chem. Theory Comput. 2013, 9, 4035−4045

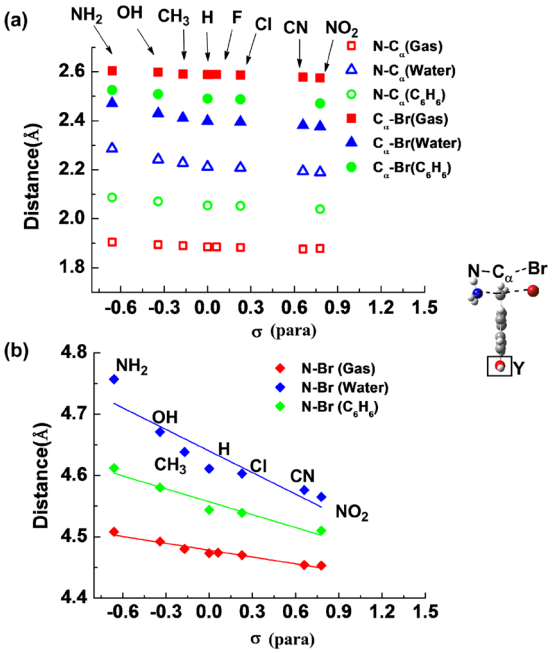

Figure 9. Relationship of the (a) N···C_α and C_α···Br distances, and (b) N···Br distances of the systems with the Hammett parameter (σ) of para-substituent Y in different solutions.

($\Delta E^{\ddagger}_{strain}$) and the T-S interaction energy ($\Delta E^{\ddagger}_{in}$). $\Delta E^{\ddagger}_{strain}$ is related to the structural deformation from the equilibrium reactants to the separated structures that form in the transition state. The influence on geometrical structure deformation by the para-substituent effects is associated with $\Delta E^{\ddagger}_{strain}$. As shown in Table 4, $\Delta E^{\ddagger}_{strain}$ increased when the substituents (Y) became more electron-withdrawing. This implies that para-substituted benzyl bromides (with electron-withdrawing substituents) were significantly more deformed. $\Delta E^{\ddagger}_{in}$ also increased when Y became more electron-withdrawing in these reactions. These corresponding $\Delta E^{\ddagger}_{strain}$ and $\Delta E^{\ddagger}_{in}$ values made $\Delta E^{\ddagger}$ lower than that of unsubstituted benzyl bromide. This trend could also be observed in benzene and water. However, the specific orbital interaction contribution from the para-substituents was still unclear from the present analysis; thus, we used our TS/TB-PCM method to estimate the specific interactions from the substituents Y in the following section.

TS/TB Orbital Interaction Analysis of the Substituent Effects on the Activation Energy in Gas and Solution. Stereoelectronic effects were investigated by the TS/TB orbital interaction analysis[11] in our previous study. The orbital interactions in solutions may give more important insight into the mechanisms of the Menshutkin reactions, as many organic reactions occur in solutions. Thus, our TS/TB-PCM method is useful for mechanistic investigations in solutions. Substituents at the para position change the magnitude of the electron transfer from the entire substituted phenyl ring ($-C_6H_4Y$) by tuning the electron interactions during the reaction, as shown in the above discussions. We deleted some specific orbital interactions from the substituents to determine the key contributing interactions. The structures optimized at PCM/MP2 from GAUSSIAN 09 are selected for the TS/TB orbital interaction analysis. The contribution from orbital interactions (ΔE) is defined as $\Delta E = E_a - E_a'$, where E_a is the activation energy without orbital interaction deletion, and E_a' is the activation energy after deletion.

Our objection was to examine concrete interactions that lower the activation energy on the system where Y = H by substituents such as Y = NH_2 or NO_2. Table 5 shows the important orbital interaction contributions that affect the activation energy. For the system with Y = NH_2, the lone-pair electrons from the N atom were expected to strongly interact with the π orbitals from the phenyl group (see Figure 10b). The orbital interaction between the lone-pair electron orbital in the N atom and the π^* orbital in the ph, $n(NH_2)-\pi^*(ph)$, was deleted by the TS/TB-PCM method to estimate its contributions. The analysis showed that E_a increased by 0.29, 0.22, and 0.89 kcal/mol after the interaction of $n(NH_2)-\pi^*(ph)$ was deleted in gas, benzene, and water, respectively. In other words, the activation energy after the deletion became similar to that of the system with Y = H, because the interaction of $n(NH_2)-\pi^*(ph)$ that is inherently missing in the system with Y = H was deleted in the system with Y = NH_2. For an easier comparison, the effects of orbital interactions of the substituents on the activation energies are compared in Figure 11. In water, the activation energy of the structure with Y = NH_2 was ~0.68 kcal/mol (= 16.83 kcal/mol − 16.15 kcal/mol) lower than that of the structure with Y = H (Figure 11). Obviously, the interactions of $n(NH_2)-\pi^*(ph)$ in water (0.89 kcal/mol) are much stronger than those in gas (0.29 kcal/mol) and in benzene (0.22 kcal/mol) (see Table 5). The activation energy increased to 17.04 kcal/mol, which is similar to that of unsubstituted benzyl bromide (16.83 kcal/mol), by deleting the interaction between NH_2 and the phenyl ring, as shown in Figure 11a. On the other hand, for the system

Table 4. Strain Energy ($\Delta E^{\ddagger}_{strain}$),[a] Interaction Energy ($\Delta E^{\ddagger}_{in}$),[b] and the Activation Energy ($\Delta E^{\ddagger}$)[c] Calculated from $\Delta E^{\ddagger} = \Delta E^{\ddagger}_{strain} + \Delta E^{\ddagger}_{in}$ at the MP2/6-31+G(d) Level

	In Gas (kcal/mol)			In Water (kcal/mol)			In Benzene (kcal/mol)		
Y	$\Delta E^{\ddagger}_{strain}$	$\Delta E^{\ddagger}_{in}$	$\Delta E^{\ddagger}$	$\Delta E^{\ddagger}_{strain}$	$\Delta E^{\ddagger}_{in}$	$\Delta E^{\ddagger}$	$\Delta E^{\ddagger}_{strain}$	$\Delta E^{\ddagger}_{in}$	$\Delta E^{\ddagger}$
NH_2	36.27	−9.97	26.31	15.03	−1.66	13.37	24.26	−5.95	18.31
OH	37.70	−10.84	26.86	15.90	−2.04	13.87	25.58	−6.62	18.95
CH_3	37.86	−11.42	26.43	15.89	−2.13	13.76	25.62	−6.88	18.74
H	38.84	−12.10	26.74	16.48	−2.53	13.95	26.41	−7.43	18.99
F	39.12	−12.04	27.07	16.55	−2.42	14.13	26.65	−7.50	19.15
Cl	39.00	−12.33	26.67	16.51	−2.48	14.03	26.37	−7.53	18.84
CN	39.95	−13.69	26.27	16.68	−2.77	13.92	27.06	−8.31	18.75
NO_2	40.06	−13.96	26.10	16.84	−2.92	13.92	27.21	−8.56	18.65

[a] $\Delta E^{\ddagger}_{strain} = (E(NH_3)_{deformed} + E(CH_2Br(C_6H_4Y))_{deformed}) - (E(NH_3)_{opt} + E(CH_2Br(C_6H_4Y))_{opt})$. [b] $\Delta E^{\ddagger}_{in} = E(T\text{-}S) - (E(NH_3)_{deformed} + E(CH_2Br(C_6H_4Y))_{deformed})$. [c] $\Delta E^{\ddagger} = \Delta E^{\ddagger}_{strain} + \Delta E^{\ddagger}_{in}$.

dx.doi.org/10.1021/ct4006163 | J. Chem. Theory Comput. 2013, 9, 4035−4045

Table 5. Orbital Contributions (ΔE) to the Activation Energy of Para-substituted Benzyl Bromides by the TS/TB-PCM Method at the MP2/6-31+G(d) Level

Y	deletion of orbital interactions[a]	ΔE (kcal/mol)[b] gas	benzene	water
NH_2	$n(NH_2)-\pi^*(ph)$	+0.29	+0.22	+0.89
	$\pi^*(ph)-\sigma^*(C_\alpha-Br)$	c	+3.58	+4.07
NO_2	$\pi(NO_2)-\pi^*(ph)$	−0.30	−0.36	−0.56
	$\pi(ph)-\pi^*(NO_2)$	−0.36	−0.08	+0.49
	$n(O)-\sigma^*(N-C)$	+0.23	+0.11	−0.19
	$\pi(NO_2)-\pi^*(ph)$ and $\pi(ph)-\pi^*(NO_2)$ and $n(O)-\sigma^*(N-C)$	−0.29	+0.17	+0.36
	$\pi^*(ph)-\sigma^*(C_\alpha-Br)$	c	+1.78	+3.78
H	$\pi^*(ph)-\sigma^*(C_\alpha-Br)$	c	+2.02	+2.87

[a] n = lone-pair electron orbital. [b] $\Delta E = E_a - E_a'$. E_a: activation energy without orbital interaction deletion. E_a': activation energy after orbital interaction deletion. Negative sign(−): After orbital deletion, the activation energy barrier becomes lower. Positive sign(+): After orbital deletion, the activation energy barrier becomes higher. [c] The interaction was not compared.

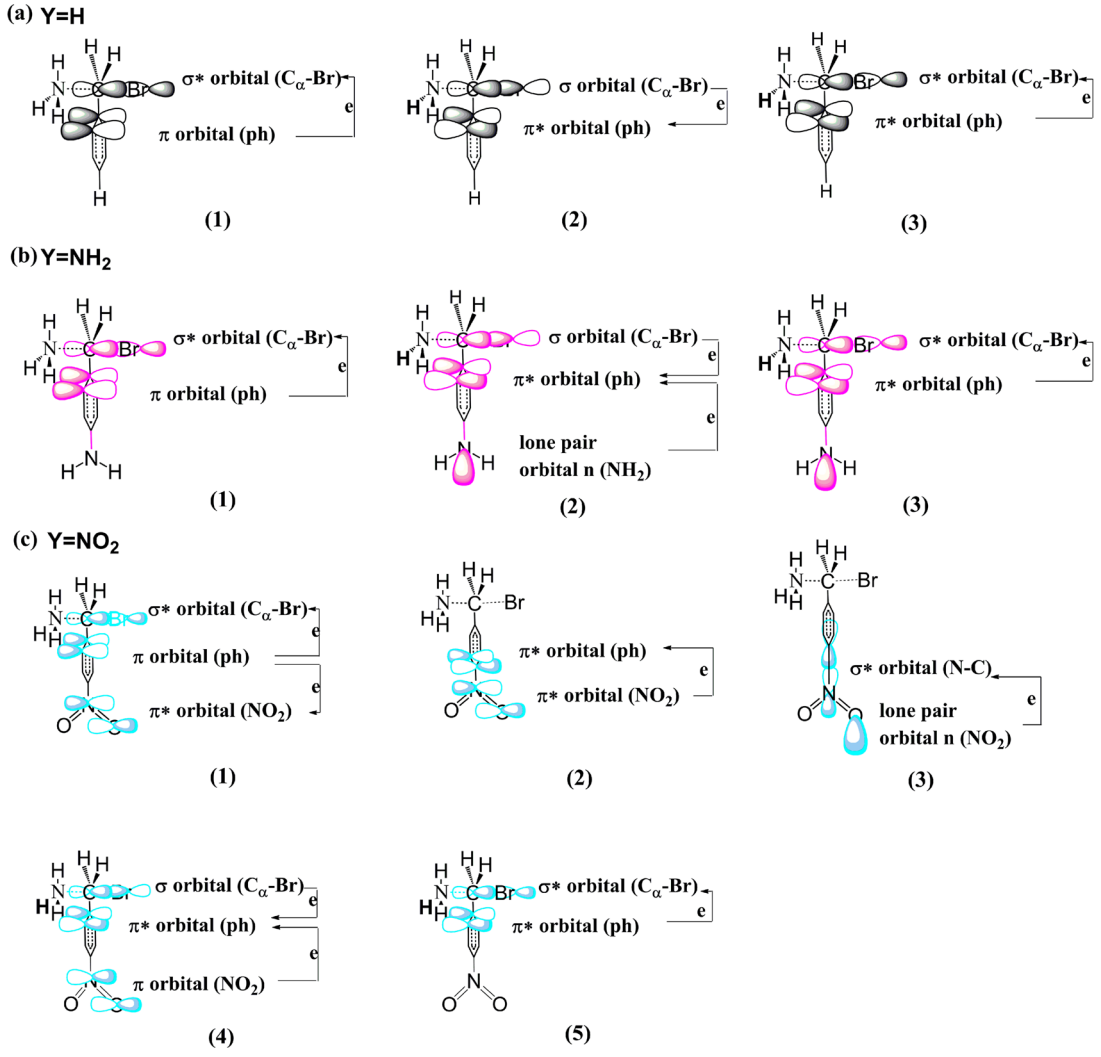

Figure 10. Some important orbital interactions in systems with (a) Y = H, (b) Y = NH_2, and (c) Y = NO_2.

with Y = NO_2, the key orbital interactions were not as simple to discern. There were various possible orbital interactions to consider, such as the interactions between the π orbitals in the ph group with the double bond N═O orbital (see (**1**), (**2**), and (**4**) in Figure 10c) and the lone-pair electron orbitals in the N and O atoms of the NO_2 group (see (**3**) in Figure 10c). For three important interactions listed in Table 5, the contributions to the activation energy E_a were calculated. The change of the energy barrier after the deletion of $\pi(ph)-\pi^*(NO_2)$, $\pi(NO_2)$-$\pi^*(ph)$, and $n(O)-\sigma^*(N-C)$ was not directly equal to the

dx.doi.org/10.1021/ct4006163 | J. Chem. Theory Comput. 2013, 9, 4035−4045

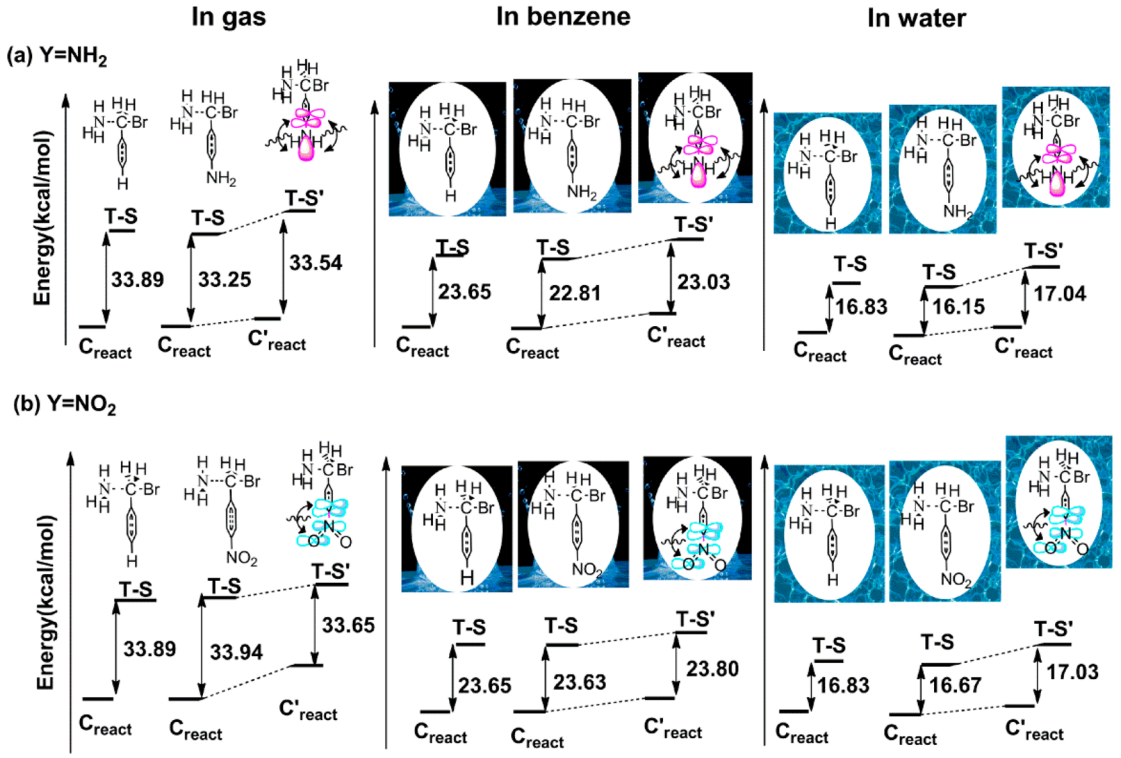

Figure 11. Comparison of activation energies of the systems with substituents (a) Y = NH_2 (b) Y = NO_2 after orbital deletions with those of the systems with Y = H in gas, in benzene, and in water.

summation of the remaining interactions, because there were some overlaps between these orbital interactions. However, the analysis can predict the key orbital interactions and estimate the change in E_a by deleting each of the orbital interactions. In water, the key orbital interaction was found to be the π(ph)−π^*(NO_2) interaction ((**1**) in Figure 10c), which lowered the E_a barrier by ∼0.49 kcal/mol. However, the π(ph)−π^*(NO_2) interaction increased the E_a value in the gas phase (−0.36 kcal/mol) and in benzene (−0.08 kcal/mol). In contrast, the interaction of n(O)−σ^*(N−C) ((**3**) in Figure 10c) contributed to lowering the E_a value in the gas phase and in benzene. As shown in Table 5, the E_a values decreased (negative values) or increased (positive values) by −0.29, 0.17, and 0.36 kcal/mol after the interactions between the NO_2 group and ph group were deleted in the gas phase, in benzene, and in water, respectively. These effects can be more easily compared in Figure 11b. The E_a' value decreased (33.65 kcal/mol) in the gas phase. Conversely, it increased (17.03 kcal/mol) in water after the deletions. All of the activation energies (E_a') were similar to those of unsubstituted benzyl bromide when the orbital interactions were deleted from the systems.

There is an explanation of the role of Y in tuning the orbital interaction between phenyl and C_α. For the system with Y = H, as shown in Figure 10a, there are possibilities of the electron transfer from the σ orbital of C_α−Br to the π^* orbitals of the ph group (see (**1**) in Figure 10a) and from the π orbitals of the ph group to the σ^* orbital of C_α−Br (see (**2**) in Figure 10a) in delocalizing benzyl bromide. Moreover, there may be electronic orbital interactions from the π^* orbitals of the ph group to the σ^* orbital of C_α−Br (see (**3**) in Figure 10a). All of these electron interactions (σ(C_α−Br)−π^*(ph), π(ph)−σ^*(C_α−Br), and π^*(ph)−σ^*(C_α−Br)) stabilized the transition states. Considered as an inner-sphere electron-transfer reaction,[20] the Menshutkin reaction is the progress of electron transfer from the nucleophile NH_3 to the leaving group Br. For the system with Y = NH_2, the n(NH_2)−π^*(ph) interaction (see (**2**) in Figure 10b) enhanced the possibility of π^*(ph)−σ^*(C_α−Br) interactions (see (**3**) in Figure 10b); the electron orbital interaction from π^*(ph) to σ^*(C_α−Br) will become stronger when the π^*(ph) orbital receives more electrons from the N atom. For the system with Y = NO_2 (Figure 10c), compared with the π(NO_2)−π^*(ph) interaction ((**4**) in Figure 10c), the π(ph)−π^*(NO_2) interaction (shown in (**1**)) is the key factor for lowering the activation energy barrier in water; this can be explained because the electron-withdrawing ability of the N═O bond in the NO_2 group is stronger than the C═C bond in ph. It is worthwhile to point out that the π^*(NO_2)−π^*(ph) interaction of (**2**) can also occur during the reaction. This interaction compensates for some electrons in π^*(ph) and enhances the electron transfer from the π^*(ph) to the σ^*(C_α−Br) orbital. As shown in Table 5, the contributions of the interaction π^*(ph)−σ^*(C_α−Br) were 2.87, 4.07, and 3.78 kcal/mol for the systems with Y = H, Y = NH_2, and Y = NO_2, respectively. The above discussions indicate that stronger interactions between π^*(ph) and σ^*(C_α−Br) orbitals occur when introducing the para-substituents −NH_2 and −NO_2. This stronger interaction stabilizes the transition state and forces the leaving group Br to leave more easily.

Although the contributions of orbital interactions are slightly overestimated in water, this study provides evidence that the TS/TB orbital interaction analysis can predict the substituent effects on reactions by evaluating orbital interaction contributions. We believe that our approach in this study sheds light on the control of S_N2 reactions.

dx.doi.org/10.1021/ct4006163 | J. Chem. Theory Comput. 2013, 9, 4035−4045

CONCLUSION

In this study, we developed the through-space/bond (TS/TB)−PCM method to interpret the mechanism of acceleration for S_N2 reactions from the orbital interaction perspective in solutions. The presentation of the substituent effects depends on the level of theory. The electron correlation effect, as well as the diffusion functions in the basis set, significantly affect the determination of the substituent effects on the reactivity of para-substituted benzyl bromide in S_N2 reactions. The $-C_6H_4Y$ groups receive negative charges through the reaction process, based on "relative reduced charge" calculations, and both electron-donating and electron-withdrawing substituents Y facilitate greater charges. The electron-transfer activities of the whole $-C_6H_4Y$ group indicated that the activation energy barriers decrease when the electron-transfer activities become stronger around the central carbon. The T-S structures became looser in solutions, especially in polar solvent water. The calculations may predict that polar solvents induce the formation of the transition states (T-S(s)) more easily. The TS/TB-PCM analysis showed that the key orbital interactions for stabilizing the T-S(s) in water are $n(NH_2)-\pi^*(ph)$ for the system with Y = NH_2 and $\pi(ph)-\pi^*(NO_2)$ for the system with Y = NO_2. In benzyl bromide, the $\sigma(C_\alpha-Br)-\pi^*(ph)$, $\pi(ph)-\sigma^*(C_\alpha-Br)$, and $\pi^*(ph)-\sigma^*(C_\alpha-Br)$ interactions contribute to the stabilization of the T-S(s). Substituents NH_2 and NO_2 enhance the interaction of $\pi^*(ph)-\sigma^*(C_\alpha-Br)$, which enables the leaving group Br to leave more easily. In conclusion, our findings give us evidence that the TS/TB orbital interaction analysis can predict the substituent effects in solutions by evaluating the orbital interaction contributions.

ASSOCIATED CONTENT

Supporting Information

Details regarding the activation energies calculated at different levels, and the activation energies of para-substituted benzyl bromide structures with thermal corrections. This material is available free of charge via the Internet at http://pubs.acs.org.

AUTHOR INFORMATION

Corresponding Author

*E-mail: aoki.yuriko.397@m.kyushu-u.ac.jp.

Notes

The authors declare no competing financial interest.

ACKNOWLEDGMENTS

This study was supported by a grant-in-aid from the Ministry of Education, Culture, Sports, Science, and Technology of Japan (MEXT). L.J. is grateful for a scholarship from MEXT associated with the launch of the Global 30 Project. Calculations were performed on systems in our laboratory, which included Linux PCs.

REFERENCES

(1) Hoffmann, R.; Imamura, A.; Hehre, W. J. *J. Am. Chem. Soc.* **1968**, *90*, 1499−1509.
(2) Hoffmann, R. *Acc. Chem. Res.* **1971**, *4*, 1−9.
(3) Doerner, T.; Gleiter, R.; Robbins, T. A.; Chayangkoon, P.; Lightner, D. A. *J. Am. Chem. Soc.* **1992**, *114*, 3235−3241.
(4) Schafer, O.; Allan, M.; Szeimies, G.; Sanktjohanser, M. *Chem. Phys. Lett.* **1992**, *195*, 293−297.
(5) Scholes, G. D.; Ghiggino, K. P.; Oliver, A. M.; Paddonrow, M. N. *J. Am. Chem. Soc.* **1993**, *115*, 4345−4349.
(6) Clayton, A. H. A.; Scholes, G. D.; Ghiggino, K. P.; PaddonRow, M. N. *J. Phys. Chem.* **1996**, *100*, 10912−10918.
(7) Imamura, A.; Sugiyama, H.; Orimoto, Y.; Aoki, Y. *Int. J. Quantum Chem.* **1999**, *74*, 761−768.
(8) Oosterbaan, W. D.; Havenith, R. W. A.; van Walree, C. A.; Jenneskens, L. W.; Gleiter, R.; Kooijman, H.; Spek, A. L. *J. Chem. Soc., Perkin Trans. 2* **2001**, 1066−1074.
(9) Orimoto, Y.; Aoki, Y. *Int. J. Quantum Chem.* **2003**, *92*, 355−366.
(10) Sun, D. L.; Rosokha, S. V.; Lindeman, S. V.; Kochi, J. K. *J. Am. Chem. Soc.* **2003**, *125*, 15950−15963.
(11) Orimoto, Y.; Naka, K.; Aoki, Y. *Int. J. Quantum Chem.* **2005**, *104*, 911−918.
(12) Sobczyk, M.; Neff, D.; Simons, J. *Int. J. Mass Spectrom.* **2008**, *269*, 149−164.
(13) Orimoto, Y.; Imai, T.; Naka, K.; Aoki, Y. *J. Phys. Chem. A* **2006**, *110*, 5803−5808.
(14) Boman, P.; Eliasson, B.; Grimm, R. A.; Staley, S. W. *J. Chem. Soc., Perkin Trans. 2* **2001**, 1130−1138.
(15) Weiss, E. A.; Sinks, L. E.; Lukas, A. S.; Chernick, E. T.; Ratner, M. A.; Wasielewski, M. R. *J. Phys. Chem. B* **2004**, *108*, 10309−10316.
(16) Neff, D.; Sobczyk, M.; Simons, J. *Int. J. Mass Spectrom.* **2008**, *276*, 91−101.
(17) Cho, H. S.; Jeong, D. H.; Yoon, M. C.; Kim, Y. H.; Kim, Y. R.; Kim, D.; Jeoung, S. C.; Kim, S. K.; Aratani, N.; Shinmori, H.; Osuka, A. *J. Phys. Chem. A* **2001**, *105*, 4200−4210.
(18) Kurlancheek, W.; Cave, R. J. *J. Phys. Chem. A* **2006**, *110*, 14018−14028.
(19) Reed, A. E.; Weinhold, F. *Isr. J. Chem.* **1991**, *31*, 277−285.
(20) Sola, M.; Lledos, A.; Duran, M.; Bertran, J.; Abboud, J. L. M. *J. Am. Chem. Soc.* **1991**, *113*, 2873−2879.
(21) Xing, Y. M.; Xu, X. F.; Chen, L.; Cai, Z. S.; Zhao, X. Z.; Cheng, J. P. *Phys. Chem. Chem. Phys.* **2002**, *4*, 4669−4677.
(22) Vayner, G.; Houk, K. N.; Jorgensen, W. L.; Brauman, J. I. *J. Am. Chem. Soc.* **2004**, *126*, 9054−9058.
(23) Pliego, J. R. *J. Mol. Catal. A: Chem.* **2005**, *239*, 228−234.
(24) Streitwieser, A.; Jayasree, E. G. *J. Org. Chem.* **2007**, *72*, 1785−1798.
(25) Garver, J. M.; Fang, Y. R.; Eyet, N.; Villano, S. M.; Bierbaum, V. M.; Westaway, K. C. *J. Am. Chem. Soc.* **2010**, *132*, 3808−3814.
(26) Liang, J. X.; Geng, Z. Y.; Wang, Y. C. *J. Comput. Chem.* **2012**, *33*, 595−606.
(27) Valero, R.; Song, L. C.; Gao, J. L.; Truhlar, D. G. *J. Chem. Theory Comput.* **2009**, *5*, 1−22.
(28) Sauers, R. R. *J. Chem. Theory Comput.* **2010**, *6*, 602−606.
(29) Geerke, D. P.; Thiel, S.; Thiel, W.; van Gunsteren, W. F. *J. Chem. Theory Comput.* **2007**, *3*, 1499−1509.
(30) Chandrasekhar, J.; Smith, S. F.; Jorgensen, W. L. *J. Am. Chem. Soc.* **1984**, *106*, 3049−3050.
(31) Acevedo, O.; Jorgensen, W. L. *J. Phys. Chem. B* **2010**, *114*, 8425−8430.
(32) Kostal, J.; Voutchkova, A. M.; Jorgensen, W. L. *Org. Lett.* **2012**, *14*, 260−263.
(33) Pu, J. Z.; Truhlar, D. G. *J. Phys. Chem. A* **2005**, *109*, 773−778.
(34) Papajak, E.; Truhlar, D. G. *J. Chem. Phys.* **2012**, 137.
(35) Zhao, Y.; Truhlar, D. G. *J. Chem. Theory Comput.* **2010**, *6*, 1104−1108.
(36) Craig, S. L.; Brauman, J. I. *Science* **1997**, *276*, 1536−1538.
(37) Kirby, A. J. *Stereoelectronic Effects*; Oxford University: Oxford, U.K., 1996.
(38) Westaway, K. C.; Waszczylo, Z. *Can. J. Chem.* **1982**, *60*, 2500−2520.
(39) Gao, J. L.; Xia, X. F. *J. Am. Chem. Soc.* **1993**, *115*, 9667−9675.
(40) Abboud, J.-L. M.; Notario, R.; Bertrán, J.; Solà, M. *Prog. Phys. Org. Chem.* **1993**, *19*, 1−182.
(41) Pomelli, C. S.; Tomasi, J. *J. Phys. Chem. A* **1997**, *101*, 3561−3568.
(42) Mineva, T.; Russo, N.; Sicilia, E. *J. Comput. Chem.* **1998**, *19*, 290−299.

(43) Castejon, H.; Wiberg, K. B. *J. Am. Chem. Soc.* **1999**, *121*, 2139−2146.
(44) Song, L. C.; Wu, W.; Hiberty, P. C.; Shaik, S. *Chem.—Eur. J.* **2006**, *12*, 7458−7466.
(45) Su, P. F.; Ying, F. M.; Wu, W.; Hiberty, P. C.; Shaik, S. *ChemPhysChem* **2007**, *8*, 2603−2614.
(46) Poater, J.; Sola, M.; Duran, M.; Fradera, X. *J. Phys. Chem. A* **2001**, *105*, 6249−6257.
(47) Schmidt, M. W.; Baldridge, K. K.; Boatz, J. A.; Elbert, S. T.; Gordon, M. S.; Jensen, J. H.; Koseki, S.; Matsunaga, N.; Nguyen, K. A.; Su, S. J.; Windus, T. L.; Dupuis, M.; Montgomery, J. A. *J. Comput. Chem.* **1993**, *14*, 1347−1363.
(48) Mennucci, B.; Tomasi, J.; Cammi, R.; Cheeseman, J. R.; Frisch, M. J.; Devlin, F. J.; Gabriel, S.; Stephens, P. J. *J. Phys. Chem. A* **2002**, *106*, 6102−6113.
(49) Mennucci, B.; Cances, E.; Tomasi, J. *J. Phys. Chem. B* **1997**, *101*, 10506−10517.
(50) Cances, E.; Mennucci, B.; Tomasi, J. *J. Chem. Phys.* **1997**, *107*, 3032−3041.
(51) Orimoto, Y.; Naka, K.; Aoki, Y. *Int. J. Quantum Chem.* **2005**, *104*, 911−918.
(52) de Jong, G. T.; Bickelhaupt, F. M. *J. Chem. Theory Comput.* **2007**, *3*, 514−529.
(53) van Zeist, W. J.; Bickelhaupt, F. M. *Org. Biomol. Chem.* **2010**, *8*, 3118−3127.
(54) Bickelhaupt, F. M. *J. Comput. Chem.* **1999**, *20*, 114−128.
(55) Frisch, M. J.; Trucks, G. W.; Schlegel, H. B.; Scuseria, G. E.; Robb, M. A.; Cheeseman, J. R.; Scalmani, G.; Barone, V.; Mennucci, B.; Petersson, G. A.; Nakatsuji, H.; Caricato, M.; Li, X.; Hratchian, H. P.; Izmaylov, A. F.; Bloino, J.; Zheng, G.; Sonnenberg, J. L.; Hada, M.; Ehara, M.; Toyota, K.; Fukuda, R.; Hasegawa, J.; Ishida, M.; Nakajima, T.; Honda, Y.; Kitao, O.; Nakai, H.; Vreven, T.; Montgomery, J. A., Jr.; Peralta, J. E.; Ogliaro, F.; Bearpark, M.; Heyd, J. J.; Brothers, E.; Kudin, K. N.; Staroverov, V. N.; Kobayashi, R.; Normand, J.; Raghavachari, K.; Rendell, A.; Burant, J. C.; Iyengar, S. S.; Tomasi, J.; Cossi, M.; Rega, N.; Millam, J. M.; Klene, M.; Knox, J. E.; Cross, J. B.; Bakken, V.; Adamo, C.; Jaramillo, J.; Gomperts, R.; Stratmann, R. E.; Yazyev, O.; Austin, A. J.; Cammi, R.; Pomelli, C.; Ochterski, J. W.; Martin, R. L.; Morokuma, K.; Zakrzewski, V. G.; Voth, G. A.; Salvador, P.; Dannenberg, J. J.; Dapprich, S.; Daniels, A. D.; Farkas, O.; Foresman, J. B.; Ortiz, J. V.; Cioslowski, J.; Fox, D. J. *Gaussian 09, revision A.02*; Gaussian, Inc.: Wallingford, CT, 2010.
(56) Papajak, E.; Truhlar, D. G. *J. Chem. Theory Comput.* **2011**, *7*, 10−18.
(57) Hammett, L. P. *J. Am. Chem. Soc.* **1937**, *59*, 96−103.
(58) Lee, I.; Kim, C. K.; Chung, D. S.; Lee, B. S. *J. Org. Chem.* **1994**, *59*, 4490−4494.
(59) Dodd, J. A.; Brauman, J. I. *J. Phys. Chem.* **1986**, *90*, 3559−3562.
(60) Streitwieser, A.; Jayasree, E. G.; Leung, S. S. H.; Choy, G. S. C. *J. Org. Chem.* **2005**, *70*, 8486−8491.
(61) Ebrahimi, A.; Habibi-Khorassani, S. M.; Doosti, M. *Int. J. Quantum Chem.* **2011**, *111*, 1013−1024.
(62) Hammond, G. S.; Hogle, D. H. *J. Am. Chem. Soc.* **1955**, *77*, 338−340.